soil systems

MDPI

Article

Soil CO_2 Efflux in a Humid Subtropical Urban Ecosystem with Recently Transformed Soils: Seasonal Dynamics, Temperature Sensitivity and Annual Budget (Sirius Federal Territory, Russia)

Pavel Nikolaevich Skripnikov [1,2,*], Sergey Nikolaevich Gorbov [1], Ilia Pavlovich Lobzenko [1], Suleiman Samidinovich Tagiverdiev [1,2], Nadezhda Vladimirovna Salnik [1,2], Kristina Andreevna Tsymerskaya [1] and Maksim Olegovich Kravchenko [1]

[1] International Scientific Center for Ecology and Climate Change, Sirius University of Science and Technology, Krasnodar Region, 354340 Sirius Federal Territory, Russia; gorbov.sn@talantiuspeh.ru (S.N.G.); lobzenko.ip@talantiuspeh.ru (I.P.L.); 2s-t@mail.ru (S.S.T.); salnik.nv@talantiuspeh.ru (N.V.S.); tsymerskaya.ka@talantiuspeh.ru (K.A.T.); kravchenko.mo@talantiuspeh.ru (M.O.K.)
[2] D.I. Ivanovsky Academy of Biology and Medicine, Southern Federal University, 344090 Rostov-on-Don, Russia
* Correspondence: skripnikov.pn@talantiuspeh.ru

Abstract

This study quantifies the seasonal dynamics of soil CO_2 efflux in park and recreational areas of the Sirius Federal Territory, an unusual humid subtropical urban ecosystem on the Russian Black Sea coast. The territory combines a mild, humid coastal climate with rapid and extensive soil transformation during Olympic infrastructure development in 2008–2014. Monitoring was conducted at 11 sites from February to December 2025, with soil CO_2 efflux, temperature, and moisture measured twice monthly using a closed-chamber method. CO_2 efflux showed a pronounced unimodal seasonal cycle, increasing from 1.75 g C m^{-2} day^{-1} in December to 7.97 g C m^{-2} day^{-1} in July. Soil temperature was the principal abiotic correlate of flux variability, whereas soil moisture did not significantly limit respiration. The pooled Q_{10} was 1.48 (95% CI 1.42–1.55; site-specific values 1.35–1.65). Absolute differences among sites were largest in summer, but they scaled with mean flux, and no seasonal change in relative between-site variation was detected. The estimated annual CO_2 flux from the unsealed portion of the territory was 1744 g C m^{-2} yr^{-1} (95% bootstrap CI 1601–1920), corresponding to about 8322 t C yr^{-1} (7642–9164), or 30,514 t CO_2 yr^{-1}, over 477.3 ha under an assumed sealed fraction of 64.27%. January, which was not measured, was estimated by interpolation. The dataset provides a reference for soil CO_2 efflux in a strongly transformed, humid subtropical urban ecosystem, enabling comparison with urban ecosystems under contrasting climatic and land-use conditions.

Keywords: soil respiration; Q_{10} temperature sensitivity; soil moisture; urban soils; humid subtropics; carbon budget; anthropogenic soils; closed-chamber method

Received: 7 October 2026
Revised: 15 November 2026
Accepted: 20 November 2026
Published: 24 November 2026

Copyright: © 2026 by the authors. Licensee MDPI, Basel, Switzerland. This article is an open access article distributed under the terms and conditions of the Creative Commons Attribution (CC BY) license.

1. Introduction

Soil CO_2 emission represents one of the largest carbon fluxes in terrestrial ecosystems, estimated at 68–80 Pg C per year and greatly exceeding CO_2 emissions from fossil fuel combustion [1,2]. Even a modest change in the intensity of soil respiration can substantially affect the atmospheric CO_2 balance, which—against a backdrop of ongoing climate warming and accelerating urbanization—makes the quantitative assessment of these fluxes one of the priority tasks of contemporary biogeochemistry.

The main abiotic factors controlling the seasonal dynamics of soil CO_2 emission are temperature and soil moisture. The temperature dependence of emission is described by an exponential function characterized by the Q_{10} coefficient, which ranges from 1.3 to 3.3 across different ecosystems [1,3]. In subtropical soils of China, Q_{10} values of 1.9–3.2 have been reported, depending on land-use type. The effect of moisture is likewise nonlinear: emission is maximal at 60–80% of total water-holding capacity and is suppressed both under waterlogging and under desiccation. Jointly accounting for these two factors in regression models can explain up to 70–78% of the temporal variability in emission [1,3,4].

In addition to temporal variability, soil respiration is characterized by substantial spatial heterogeneity, which may occur across both local and landscape scales. Studies in boreal forests of Canada have shown that the spatial variability of soil CO_2 efflux at the local scale can be comparable to that observed across much larger spatial extents [5]. Spatial variation in soil respiration has also been documented across climatic zones and is related to environmental and soil properties, indicating that the magnitude of spatial heterogeneity is itself an ecologically meaningful characteristic of soil carbon fluxes [6]. Urban soils are particularly heterogeneous because urban land cover forms a mosaic of functional zones, vegetation types, management regimes, soil materials, and land-use histories. In urban soils, organic carbon content may vary 2–4 times more than in natural analogues [7], while the ratio of CO_2 emission to carbon stocks can be 2–3 times higher than in natural soils of the same climatic zone [8].

Previous studies have demonstrated that spatial heterogeneity of soil CO_2 efflux in urban ecosystems is associated with vegetation structure, soil properties, temperature, and management conditions. In a temperate urban forest in Beijing, seasonal spatial patterns of soil respiration were related to vegetation characteristics, soil moisture, and nutrient availability, with different controls operating during the growing and dormant seasons [9]. More recently, measurements across urban parks in the United States demonstrated that soil properties, vegetation structure, and soil temperature contributed to both the magnitude and temporal variation of CO_2 efflux [10]. These studies indicate that spatial and temporal variability are closely interconnected, so comparisons among sites should be interpreted in a seasonal context.

Despite extensive research on soil CO_2 efflux across temperate and tropical ecosystems, humid subtropical urban ecosystems remain comparatively less represented in the literature [11]. Humid subtropical urban ecosystems are of particular interest because mild winters and a long biologically active period may produce a seasonal regime of soil respiration that differs from that of temperate cities while simultaneously allowing local vegetation, hydrological, and management conditions to influence the spatial expression of soil respiration. Given the high sum of active temperatures (>4000 °C) [12], a longer period of biological activity and a different annual distribution of soil CO_2 efflux can be expected compared with temperate cities

On the Russian Black Sea coast, the climatic setting differs markedly from that of most of the country. Although the area lies at approximately 43° N, it falls within a narrow coastal belt of humid subtropical climate (Köppen Cfa), in which the Black Sea moderates the temperature regime, and the Greater Caucasus limits the penetration of cold air masses from the north, so that winters are mild and the biologically active period extends

https://doi.org/10.3390/soilsystems10120154

over most of the year [13]. This setting is unusual in the Russian context and differs from the temperate and steppe cities for which urban soil CO_2 efflux has been reported in Russia, such as Moscow, Kursk, and Rostov-on-Don [8,14–16].

On the Black Sea coast of Russia, soils of subtropical urban ecosystems are characterized by pronounced anthropogenic transformation, particularly within the Sirius Federal Territory (FT). The Imeretinskaya Lowland, where the Sirius FT is located, underwent large-scale development during preparations for the 2014 Winter Olympics (2008–2014), involving extensive earthworks, soil relocation, geoplastic modification, the construction of artificial embankments, and the creation of sports and recreational infrastructure. These activities substantially altered the morphological, physical, and chemical properties of the soil cover and its spatial distribution of organic carbon and stocks [17–19]. As a result, the present-day soil cover forms a heterogeneous mosaic of remnant natural soils, soils retaining agricultural legacies, and strongly transformed technogenic soils, including replantozems formed from relocated humus-accumulative horizons of Chernozems [19]. The resulting mosaic of natural, transformed, managed, and minimally disturbed sites provides an opportunity to examine how seasonal environmental forcing is expressed across contrasting urban soil settings. Quantitative studies of soil CO_2 efflux in the humid subtropics of Russia have been reported, particularly for the urban soils of Sochi, but available observations have generally been limited to specific soil types, functional zones, or a small number of seasonal sampling dates [20–22]. For example, studies of urban soils in Sochi have addressed residential and park-recreational zones in the mountainous landscape of the city and reported a high variability of CO_2 emission, averaging 48% [22]. Consequently, to our knowledge, multi-site, replicated measurements of soil CO_2 efflux covering almost the entire annual cycle at a regular sampling frequency are still lacking for the humid subtropical urban landscapes of Russia, including territories in which this climatic setting is combined with recent large-scale soil transformation. Such data are needed both as a regional reference and for comparison with other urban ecosystems.

Thus, the Sirius FT combines two features that make it an informative case study for soil CO_2 efflux in an urban ecosystem: a humid subtropical coastal climate that is unusual in the Russian context, and rapid, extensive, and recent (2008–2014) anthropogenic transformation of the soil cover. Similar combinations of climatic and land-use conditions may occur elsewhere; the value of the territory lies in the fact that both features are documented and jointly shape the present-day soil cover. Detailed multi-site monitoring across almost the entire annual cycle in such a setting can provide a reference dataset of soil CO_2 efflux for a humid subtropical urban ecosystem, for comparison with urban ecosystems under contrasting climatic and land-use conditions [6,9,10].

The contribution of this study is therefore threefold. First, it provides replicated measurements at 11 sites with contrasting soil origin, history and management, taken twice a month over eleven months, for a part of the Russian Black Sea coast where published observations are limited to specific soil types, functional zones or a small number of sampling dates [20–22]. Second, it separates the seasonal signal from differences among sites and tests how far the apparent temperature sensitivity of efflux reflects a response to temperature rather than the seasonal cycle itself. Third, it gives an annual soil CO_2 efflux estimate for the unsealed area of the territory with quantified uncertainty and explicit assumptions, which can be compared with urban ecosystems in other climatic and land-use settings. The study does not aim to identify the causes of differences among sites, because soil properties, management, and age vary simultaneously among them and were not controlled by the design.

Accordingly, the present study aimed to quantify the seasonal dynamics of soil CO_2 efflux in park and recreational areas of the Sirius Federal Territory, to provide a reference

dataset of these fluxes for a humid subtropical urban ecosystem with recently transformed soils, and to describe differences among sites over the annual cycle.

2. Materials and Methods

2.1. Study Area and Monitoring Sites

CO_2 efflux was measured at 11 monitoring sites (MS) covering the park and recreational zones of the Imeretinskaya Lowland during an 11-month monitoring period from February to December 2025, thereby covering nearly the entire annual cycle under the mild, humid subtropical conditions of the Russian Black Sea coast. A schematic map showing the location of the monitoring sites within the boundaries of the Sirius FT is presented in Figure 1.

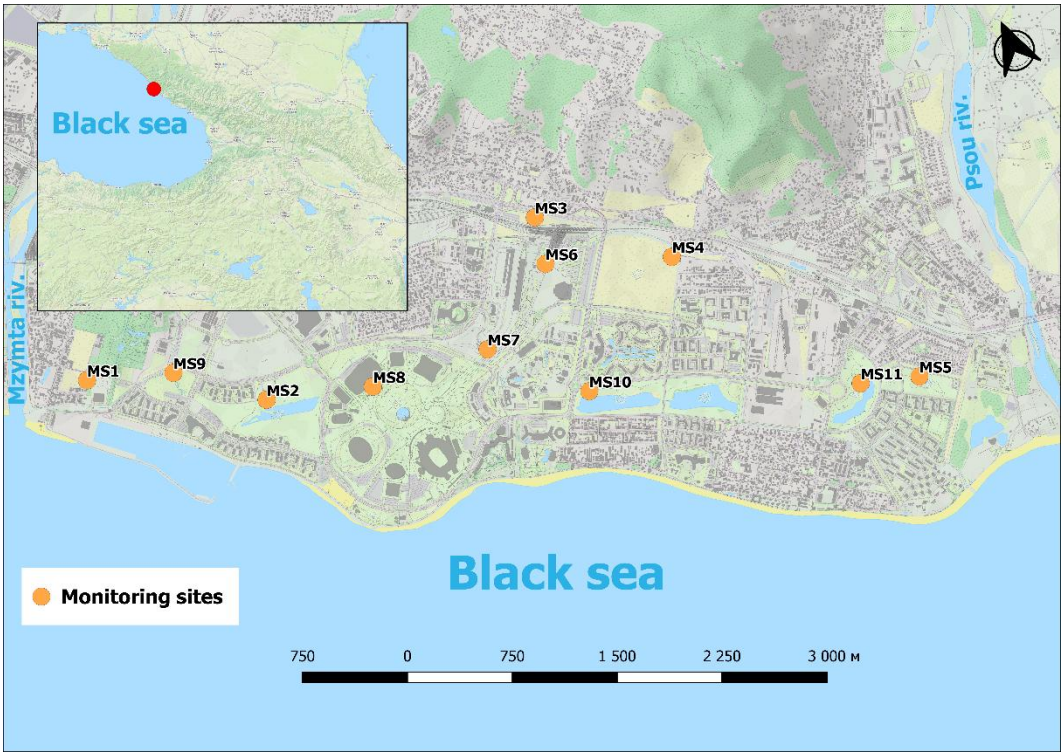


Figure 1. Schematic map of monitoring site locations.

Within the system of physical-geographical zoning, the study area belongs to the Colchis Province of the Transcaucasian Depression and, in terms of forest vegetation zoning, to the Colchis Province of subtropical forests of the Circassian District. The study area lies within the narrow humid subtropical coastal belt of the Russian Black Sea coast (Cfa according to the Köppen climate classification), characterized by abundant heat, high insolation (owing to the southwestern exposure of the lowland), and a prolonged growing season. The mean annual air temperature is +14.2 °C. Winters are mild and warm; summers are humid and hot. Precipitation is highest in the autumn–winter period [13]. In 2025, the year of the study, the annual precipitation at the Adler weather station was 1613 mm, and the mean annual air temperature was 15.1 °C [23]. Climatic characteristics refer to the Sochi area (Adler station), since the Sirius Federal Territory was formed on the territory of the former Imeretinsky resort, which was part of the Sochi agglomeration.

The relief of the Imeretinskaya Lowland is gently undulating, sloping gradually toward the Black Sea coast, with absolute elevations ranging from 1.5 to 3.0 m above sea level. The geological structure of the lowland is characterized by a mosaic of Pleistocene–Holocene deposits of diverse origin: alluvial, marsh, lacustrine, and marine. The lowland

is separated from the sea by an elevated sandy-pebble coastal ridge, while on the landward side it borders directly on hilly foothills composed of dense Paleogene–Neogene sedimentary rocks [24].

Historically, the landscapes of the Imeretinskaya Lowland comprised native Colchis forests and lowland marshes. However, over the course of the 20th century, extensive agricultural development, followed by intensive Olympic construction (2008–2014), resulted in the near-total clearance of the lowland's native forest stands and a fundamental transformation of its soil cover. Land reclamation and agricultural use erased the genetic characteristics of the soils and reduced their degree of hydromorphism. At present, this part of the study area constitutes a mosaic urban landscape with pronounced anthropogenic transformation of the soil cover [17,18].

The present-day landscape of the Imeretinskaya Lowland thus reflects two contrasting environmental legacies. First, the area lies within the humid subtropical coastal climate of the Russian Black Sea coast, where the Black Sea and the surrounding Greater Caucasus relief contribute to mild winters and limit the penetration of cold northern air masses. Second, after agricultural use during much of the twentieth century, the soil cover was subjected to rapid and extensive anthropogenic transformation during the construction of the Olympic infrastructure in 2008–2014, which involved extensive earthworks, soil relocation, geoplastic modification, and the construction of sports and recreational infrastructure. Consequently, the present-day soil cover represents a mosaic of remnant natural soils, soils with agricultural legacies, and strongly transformed technogenic soils.

The 11 monitoring sites were selected purposively rather than randomly. The aim was to cover the range of natural, abandoned, and managed park and recreational areas of the territory that differ in soil origin, history of transformation, vegetation, management, and shading, while allowing all sites to be measured on the same day with a single analyzer. The number of sites was therefore limited by the practical constraints of one-day measurements. The sites lie within the Imeretinskaya Lowland at pairwise distances of 0.35 to 5.9 km (Table 1, Figure 1). At every site, seven measurement points were used. At six sites (MS-2, MS-4, MS-5, MS-9, MS-10, and MS-11), the points were placed along the perimeter of 10 × 10 m plots established for geobotanical monitoring. At the other sites, no fixed plot size was set, and the points were placed within an area homogeneous in vegetation and relief, so that the distances between them were determined by the actual size and configuration of the area. The points are subsamples of one site and are treated as nested within sites.

The characteristics of the monitoring sites are presented in Table 1.

Table 1. Characteristics of the monitoring sites (coordinates in decimal degrees, soil names according to WRB [25]). Texture was determined in the field (rope method, Russian classification).

Site (Lat., Lon.)	Soil (WRB), Field Texture	History	Dominant Vegetation	Management	Light
MS-1 (43.4159, 39.9306)	Gleyic Fluvisols, medium loam	Fallow land next to the "Yuzhnye Kultury" arboretum, out of use since 2008, natural succession since 2009	*Platanus acerifolia, Juglans nigra, Rubus anatolicus*	None	Persistent tree-canopy shading
MS-2 (43.4100, 39.9443)	Gleyic Fluvisols, medium loam	Former agricultural land (out of use 2008), heavy machinery 2010–2012, access restricted since 2013 (Natural Park, Section 2)	*Calamagrostis pseudophragmites, Lolium multiflorum, Elymus repens*	None	Open

MS-3 (43.4133, 39.9726)	Gleyic Fluvisols, medium loam	Settlement land until 2011, railway-station construction (completed by 2014), unmaintained since 2014	*Cyperus longus, Solidago virgaurea, Rubus anatolicus*	None	Well lit
MS-4 (43.4076, 39.9822)	Urbic Technosols, light loam	Reclaimed under the "kvali" system *, temporary roads and utilities 2010–2014, not cultivated since 2014, local waterlogging	*Cyperus longus, Carex canescens, Rubus anatolicus*	None	Open
MS-5 (43.3937, 39.9974)	Urbic Technosols, medium loam	Out of use 2008, soil filling and turfing for the Olympic Games (Natural Park, Section 9)	*Paspalum dilatatum, Dactylis glomerata, Poa pratensis*	Mowing once a month	Open
MS-6 (43.4103, 39.9715)	Urbic Technosols, sandy loam	Garden created in November 2024: geotextile, Chernozem layer, sand—pebble fill, rolled turf, planted olives	*Poa pratensis turf, planted Olea europaea*	Mowing 2–3 times a month (clippings removed), fertilizers, fungicides, irrigation with a road-maintenance vehicle	Open
MS-7 (43.4068, 39.9634)	Urbic Technosols, heavy loam	Turf area in the Olympic Park, established 2013	*Paspalum dilatatum, Lolium pratense, Poa pratensis*	Mowing 2–3 times a month (clippings removed), fertilizers, fungicides, automatic irrigation	Open
MS-8 (43.4079, 39.9533)	Urbic Technosols, heavy loam	Site in the Olympic Park, formed 2012	*Poa pratensis, Paspalum dilatatum, Trifolium repens*	Mowing 2–3 times a month (clippings removed), fertilizers, fungicides, automatic irrigation	Open
MS-9 (43.4141, 39.9378)	Urbic Technosols, medium loam	Former construction area (parking, storage) established 2013 (Natural Park, Section 1)	*Eucalyptus viminalis (planted), Festuca rupicola, Lolium pratense*	Mowing once a month	Well lit
MS-10 (43.4017, 39.9704)	Urbic Technosols, heavy loam	Out of use 2008, ponds and landscape geoplasty 2011–2013 (Natural Park, Section 5)	*Paspalum dilatatum, Poa pratensis, Trifolium repens*	Mowing once a month	Well lit, shade next to the water body
MS-11 (43.3947, 39.9924)	Urbic Technosols, heavy loam	Out of use 2008, geoplasty (ponds) 2011–2013 (Natural Park, Section 7)	*Paspalum dilatatum, Trifolium repens, Dactylis glomerata*	Mowing once a month	Open, shade next to the water body

"None" means no mowing, irrigation, or fertilization. Clippings were left on the soil surface at the sites where mowing took place, except at MS-6, MS-7, and MS-8. Complete lists of dominant species are given in Table S2. * Kvali is a drainage-based melioration system formerly widespread on the former Colchis marshes of the lowland, used to drain the land and to regulate its moisture regime.

Soil properties (Table 2) were determined for the 0–10 and 10–30 cm layers. Samples were taken from soil pits located 1.8–117 m (median 13 m) from the measurement points (Table 2). The pits for MS-1, MS-2, MS-3, and MS-5 were sampled in 2024, and the others in 2025. The surface samples (0–10 cm) were taken in five replicates around the pit within 10 m, and the 10–30 cm layer was sampled in the pit. Soil organic carbon (SOC) was determined by high-temperature catalytic combustion on a Shimadzu TOC analyzer (CPN)

with an SSM-5000A solid-sample module (Shimadzu Corporation, Kyoto, Japan). Inorganic carbon was determined separately on the SSM-5000A, and SOC was calculated as total carbon minus inorganic carbon. Bulk density (BD) was measured by the volumetric core (cutting-ring) method. The pH was measured in a water suspension at a soil-to-water ratio of 1:5 with an Expert-001-3pH meter (Econix-Expert, Moscow, Russia). Soil texture was assessed in the field by the rope method and is given according to the Russian classification (Table 1). SOC stock (kg m^{-2}) was calculated for each layer as

$$SOC\ st = SOC/100 \times BD \times D \times (1 - RF/100) \times 10,$$

where SOC is in % of soil mass, BD is in g cm^{-3}, D is the layer thickness in cm, and RF is the content of rock fragments and anthropogenic inclusions (%). Stocks of the two layers were summed for 0–30 cm.

Table 2. Soil properties of the monitoring sites (0–10/10–30 cm).

Site	SOC, %	pH (H_2O, 1:5)	Bulk Density, g cm^{-3}	RF, % *	SOC Stock 0–30 cm, kg m^{-2}	Distance, m	Year of Sampling
MS-1	5.03/2.97	6.9/7.6	1.25/1.52	1.7/1.2	15.07	3.5	2024
MS-2	6.45/1.30	6.9/6.6	1.29/1.74	13.4/6.3	11.43	4.0	2024
MS-3	3.67/1.28	8.2/8.3	1.40/1.83	26.5/29.1	7.13	22.4	2024
MS-4	1.00/0.17	8.8/9.2	1.25/1.66	35.1/34.7	1.17	5.1	2025
MS-5	4.61/2.44	8.2/8.3	1.47/1.74	30.2/33.4	10.30	13.8	2024
MS-6	0.64/1.28	8.8/8.4	1.75/1.77	40.2/30.9	3.91	59.9	2025
MS-7	2.09/2.23	7.6/7.7	0.88/1.35	8.4/3.0	7.53	1.8	2025
MS-8	3.21/1.87	7.3/8.2	1.02/1.30	0.8/0.4	8.04	117	2025
MS-9	3.92/1.99	7.8/8.0	1.00/1.74	3.5/2.6	10.54	19.7	2025
MS-10	2.82/2.00	8.0/7.7	1.41/1.67	46.0/25.8	7.11	10.5	2025
MS-11	2.26/0.63	8.2/8.5	0.81/1.51	3.5/0.3	3.68	12.9	2025

* RF—rock fragments and anthropogenic inclusions. Distance—from the soil pit to the measurement points. Year is the year of soil sampling.

2.2. Measurement of CO_2 Emission

Measurements were carried out twice a month at each monitoring site, with seven replicate points per site and visit (14 per site per month) to capture within-site spatial variability. All 11 sites were measured on the same day during each visit. The replicates are subsamples of a single site rather than independent sites and were treated as nested within sites in all statistical analyses. An attempt was made to return to the same points at each visit, although exact relocation could not be guaranteed. The equipment used in the study area to measure carbon flux from the soil surface consisted of a portable EGM-5 CO_2 gas analyzer manufactured by PP Systems, equipped with a static closed chamber, together with a sensor for measuring temperature and moisture.

CO_2 flux from the soil surface was measured using the portable EGM-5 system (PP Systems, Amesbury, MA, USA) with a static closed Soil Respiration Chamber (SRC-2; PP Systems, Amesbury, MA, USA). The chamber volume was 1171 cm^3, with a soil coverage area of 78 cm^2. The duration of a single measurement was set at 120 s, with an initial delay of 9 s to allow conditions within the chamber to stabilize after installation. The CO_2 flux (FCO_2, g C m^{-2} day^{-1}) was calculated by the analyzer's software based on the change in CO_2 concentration within the chamber over time. To account for potential nonlinearities associated with micro-leaks, a quadratic approximation of the dependence of concentration (C) on time (T) was used: $C = a + bT + cT^2$. The emission rate was determined as the derivative dC/dT at time T = 0 [26].

No permanent collars were installed. Immediately before each measurement, the chamber was pressed into the soil to the depth of its cutting edge (approximately 1–2 cm), followed by the 9 s stabilization delay. Aboveground vegetation within the chamber was clipped but not removed completely, to avoid disturbing the soil surface and the growing points of herbaceous plants. The measured flux therefore represents total soil CO_2 efflux, including root and rhizosphere respiration and respiration of residual plant material, and it was not partitioned into components.

Because a single analyzer was used, the 11 sites were measured sequentially throughout daylight hours, and the exact time of each measurement was not recorded. The order of site visits was mostly constant but was occasionally changed for logistical reasons. Consequently, time of day is partly confounded with site, and diel variation in efflux is not resolved.

At the mown sites, no measurements were made on the day of mowing, and the measurements were postponed for at least one day afterwards. Dates of mowing were not recorded. Clippings were left on the soil surface at most sites and were removed only at MS-6, MS-7, and MS-8. Irrigation and the application of fertilizers and fungicides took place at MS-6, MS-7, and MS-8. No irrigation schedule was kept, and the measurements were not linked to irrigation events. No flooding of the monitoring sites was observed during the study.

In parallel with the CO_2 flux measurements, soil temperature and moisture were recorded using the system's built-in sensor. To verify the reliability of temperature readings, a digital HI98501 thermometer (Hanna Instruments, Woonsocket, RI, USA) with an accuracy of ±0.1 °C was used. Soil moisture was determined using a sensor measuring volumetric water content based on the dielectric permittivity of the soil (MC-7828 Soil; Guangzhou Landtek Instruments Co., Ltd., Guangzhou, China).

2.3. Statistical Data Processing

All statistical calculations were performed in the R statistical computing environment (version 4.6.0; R Foundation for Statistical Computing, Vienna, Austria) using the ggplot2 (v. 4.0.3), dplyr (v. 1.2.1), ggrepel (v. 0.9.8), patchwork (v. 1.3.2), lme4 (v. 2.0.1) [27], lmerTest (v. 3.2.1) [28], and emmeans (v. 2.0.3) packages.

For each site and each month, the median, interquartile range (IQR), standard deviation, and coefficient of variation of emissions were calculated. Medians were used for descriptive statistics owing to the non-normal distribution of a number of variables, and means were used for the annual budget.

Correlation analysis was performed using Spearman's coefficient (for pairwise relationships between emissions and microclimatic factors on a seasonal basis). Significance was assessed at $p < 0.05$.

The Q_{10} temperature coefficient was calculated using logarithmic linearization of the exponential dependence of emission on soil temperature. The Q_{10} value and its 95% confidence interval were determined based on the parameters of the linear regression ln(emission) ~ temperature. The calculation was performed for each site individually and for all sites combined.

Because repeated measurements within a site are not independent, the pooled Q_{10} was also estimated with a linear mixed-effects model of ln(flux) on soil temperature, with site as a random effect (random intercept and slope), $Q_{10} = \exp(10b)$. In addition, confidence intervals were calculated with standard errors clustered by site. We checked the autocorrelation of residuals between consecutive months and the normality of residuals (skewness and kurtosis). Moisture was tested by adding soil moisture and its squared term, centred within sites, to the same model.

Differences among sites were tested with the Friedman test (sites as treatments, months as blocks, February–December) with Kendall's W as effect size, and with a two-

way additive ANOVA on ln-transformed monthly site means (month and site), followed by pairwise comparisons adjusted by the Holm method. The variance of ln-transformed fluxes was partitioned among month, site, site × month interaction, and replicate measurements with a mixed model (month as a fixed effect, site and site × month as random effects).

To describe how differences among sites changed through the year, we calculated for each month the interquartile range, standard deviation, range and coefficient of variation of the 11 site medians. Because absolute dispersion increases with the mean, we also calculated the standard deviation of ln-transformed site medians. Differences among months were tested with the Friedman test on the absolute deviation of each site's median from the median of all sites (Nemenyi post hoc test), applied to both original and ln-transformed values, and the July–December contrast was tested with an exact paired Wilcoxon test. Only the 11 measured months (February–December) were used.

The relationship between soil moisture and efflux was examined by correlation analysis, quadratic regression, a generalized additive model (GAM), analysis of the residuals of the temperature model, and the mixed model described above. Because the time of measurement was not recorded, the deviation of air temperature from its visit-day mean was used as a proxy for time of day, and we tested whether including it changed differences among sites. Relationships between mean site flux and soil properties were explored with Spearman rank correlations, and mowing regimes were compared with the Kruskal–Wallis test.

Field measurements could not be carried out in January. For this month, CO_2 efflux was estimated as the mean of the December and February values (linear interpolation) and is marked as an estimate in all tables and figures.

The annual flux was calculated by summing monthly mean fluxes multiplied by the number of days in the month and scaling the result to the unsealed area of the territory. Sums based on monthly medians are reported for comparison, since right-skewed data bias median-based sums downward. Uncertainty was estimated with a two-level bootstrap (2000 resamples of sites and of replicate measurements within site and month). The total area (1335.88 ha, without water bodies) and the sealed fraction (64.27%) are described in Section 3.3.

3. Results

3.1. Seasonal Dynamics of CO_2 Emission and Differences Among Monitoring Sites

CO_2 emission from soils at the studied sites exhibited pronounced seasonal dynamics, with a clearly defined winter minimum and summer maximum. Median values (median (Q1; Q3)) across the entire set of sites ranged from 1.75 (1.49; 2.15) in December to 7.97 (6.35; 9.95) g C m^{-2} day^{-1} in July. Emission intensity during the summer peak exceeded the winter minimum by a factor of 4.6. A significant increase in fluxes began in March (4.28 (3.50; 4.91) g C m^{-2} day^{-1}), reached a maximum in July, and was followed by a gradual decline through December. The seasonal dynamics of emissions are shown visually in Figure 2. The spring rise was steep: the median flux increased 2.2-fold, from 2.53 (2.14; 3.27) g C m^{-2} day^{-1} in February to 5.57 (4.62; 6.33) g C m^{-2} day^{-1} in April.

Soil CO_2 efflux differed significantly among the 11 sites (Friedman test with months as blocks: $\chi^2 = 54.5$, df = 10, $p < 0.001$, Kendall's W = 0.50), but the differences were small compared with the seasonal variation. Month accounted for 71% of the variance of ln-transformed fluxes. Of the variance remaining after the effect of month was removed, 23% was attributable to site, 12% to the site × month interaction and 65% to replicate measurements within site and month. Annual median fluxes ranged from 3.69 g C m^{-2} day^{-1} at MS-1 to 6.16 g C m^{-2} day^{-1} at MS-10 (1.7-fold), whereas the other nine sites ranged only from 4.47 to 5.28 g C m^{-2} day^{-1} (1.18-fold, pooled median 4.86). After adjustment for month, flux

was 25% lower at MS-1 (95% CI −33 to −17%) and 39% higher at MS-10 (26 to 54%) than the geometric mean of all sites. MS-1 had the lowest flux in 10 of 11 months and MS-10 the highest in 9 of 11 (Figure 3).

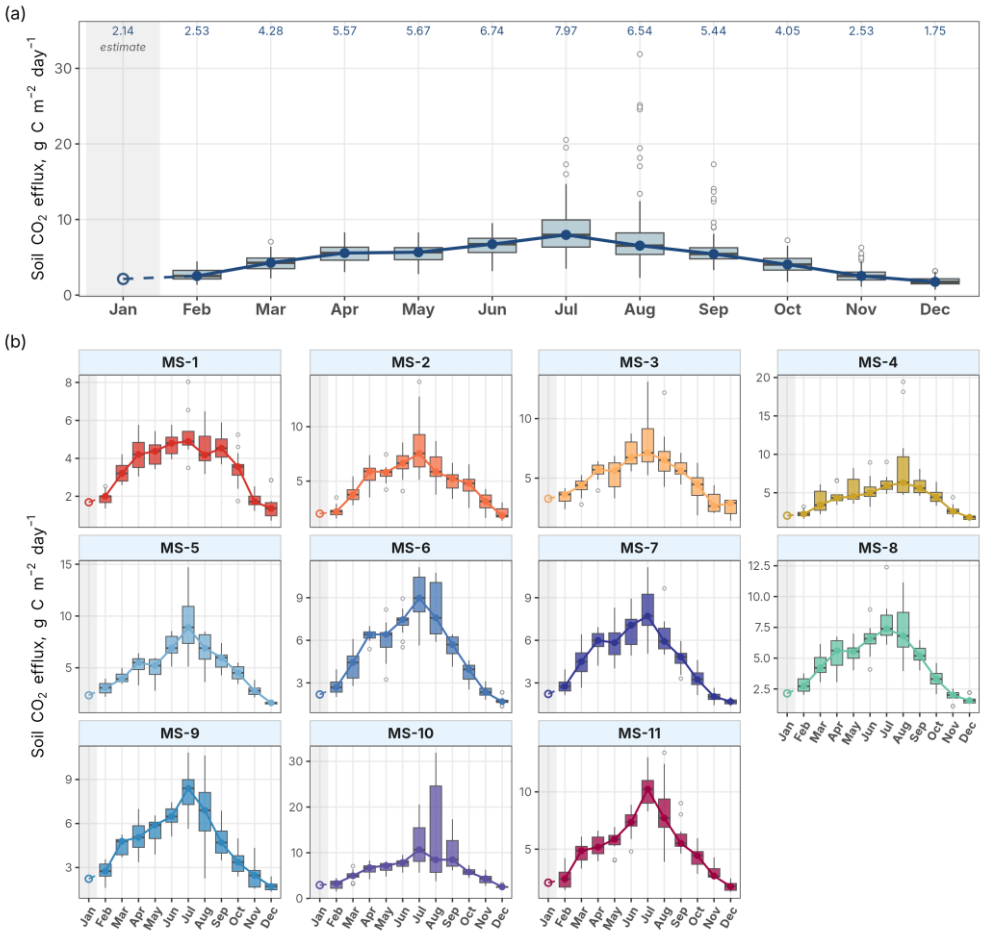


Figure 2. Seasonal dynamics of CO_2 efflux: (**a**) all sites combined and (**b**) each monitoring site. Boxes show quartiles, and lines show monthly medians. January was not measured and is estimated by interpolation (hollow marker, dashed line, and grey band). Numbers above panel (**a**) are monthly medians (g C m^{-2} day^{-1}).

All 19 significant pairwise differences (Holm-adjusted, 55 pairs) involved MS-1 or MS-10, whereas none of the 36 comparisons among the other nine sites were significant (Friedman $p = 0.13$, with a weak site effect in the two-way ANOVA, $p = 0.03$, and no significant pair). The high flux at MS-10 was most pronounced in July–September, when it was also the most variable (mean ± SD in August: 14.0 ± 10.1 g C m^{-2} day^{-1}, Table S1).

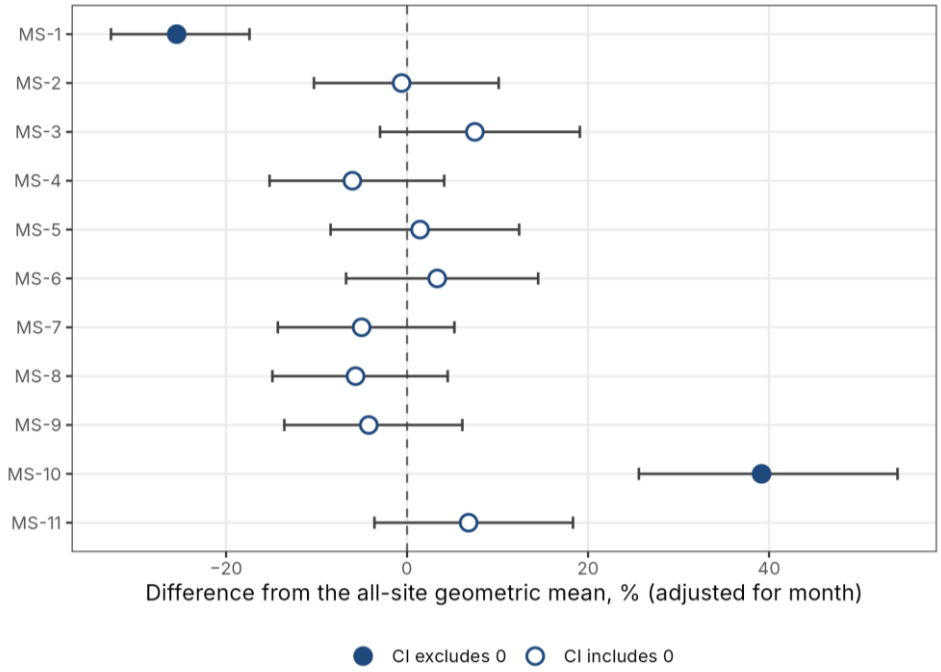


Figure 3. Differences in soil CO_2 efflux among sites after adjustment for month, as % deviation from the geometric mean of all sites (95% confidence intervals). The dashed vertical line marks zero difference, i.e., the geometric mean of all sites.

3.2. Calculation of the Q_{10} Temperature Coefficient and Analysis of the Influence of Microclimatic Factors on the Seasonal Dynamics of Emission

3.2.1. Effect of Temperature

The Q_{10} temperature coefficient, calculated by logarithmic linearization of the exponential model describing the dependence of CO_2 emission on soil temperature in the 0–1 cm layer, proved to be statistically significant for all sites and for all sites combined ($p < 0.01$ in all cases).

Across individual sites, Q_{10} values ranged from 1.35 (MS-7) to 1.65 (MS-11) (Figure 4). The lowest Q_{10} values were recorded at MS-7 (1.35) and MS-3 (1.37), and the highest at MS-11 (1.65) and MS-10 (1.62), sites that underwent geoplastic transformation and are located close to water bodies. Mean Q_{10} values by mowing regime were similar (1.49 without mowing, 1.54 monthly, 1.42 more than twice a month), and their ranges overlapped, so no effect of mowing on Q_{10} can be inferred. The coefficient of determination (R^2) ranged from 0.21 (MS-7) to 0.51 (MS-2 and MS-11), indicating that at individual sites temperature explains between 21% and 51% of emission variability, with the remainder attributable to other factors. A linear mixed-effects model with site as a random effect gave a pooled Q_{10} of 1.48 (95% CI 1.42–1.55). Residuals of consecutive months were positively autocorrelated (mean lag-1 r = 0.58), so standard errors clustered by site were also computed, giving a pooled Q_{10} of 1.49 (95% CI 1.41–1.57). The residuals were close to symmetric (skewness −0.44, excess kurtosis −0.04).

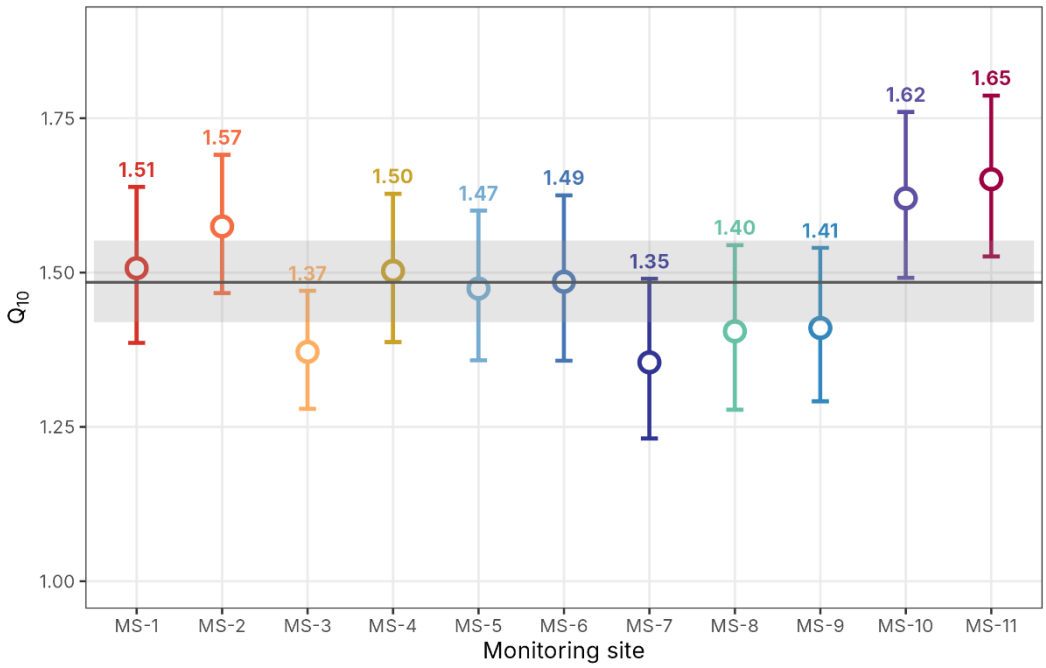


Figure 4. Q_{10} temperature coefficient for each monitoring site with 95% confidence intervals (bars). The grey horizontal line and the grey band show the pooled estimate from the mixed-effects model (1.48) and its 95% CI (1.42–1.55). All site-specific relationships were significant ($p < 0.01$).

3.2.2. Effect of Moisture

Analysis of the relationship between field soil moisture and emission intensity using Spearman rank correlation coefficients revealed no statistically significant linear relationship ($p > 0.05$) for any of the eleven monitoring sites. A quadratic regression model was subsequently constructed for the entire dataset to identify a potential nonlinear relationship. The model as a whole was not statistically significant ($p = 0.134$), and the proportion of explained variance was negligible ($R^2 = 0.0024$). An additional check using a generalized additive model (GAM) confirmed this result: the smoothing function for moisture was statistically non-significant ($p = 0.285$, deviance explained = 0.22%).

Since the temperature sensitivity of CO_2 emission (the Q_{10} coefficient) was established as a statistically significant factor for the dataset as a whole ($R^2 = 0.346$, $p < 0.001$), the final assessment of the independent contribution of moisture was based on an analysis of the residuals of the temperature model. Neither the quadratic regression ($p = 0.698$, $R^2 = 0.0004$) nor the GAM (deviance explained = 0.001%) revealed a significant dependence of the residuals on soil moisture (Figure 5).

Thus, the combined set of methods applied (quadratic regression, GAM, and analysis of temperature-model residuals) indicates the absence of a statistically significant effect of soil moisture on CO_2 emission intensity. In a linear mixed-effects model with site as a random effect, soil moisture was not significant after accounting for temperature ($p = 0.86$), and the within-site linear and quadratic moisture terms were also not significant ($p = 0.87$ and 0.34). Soil moisture varied between 35 and 69%, so the absence of an effect applies to this range.

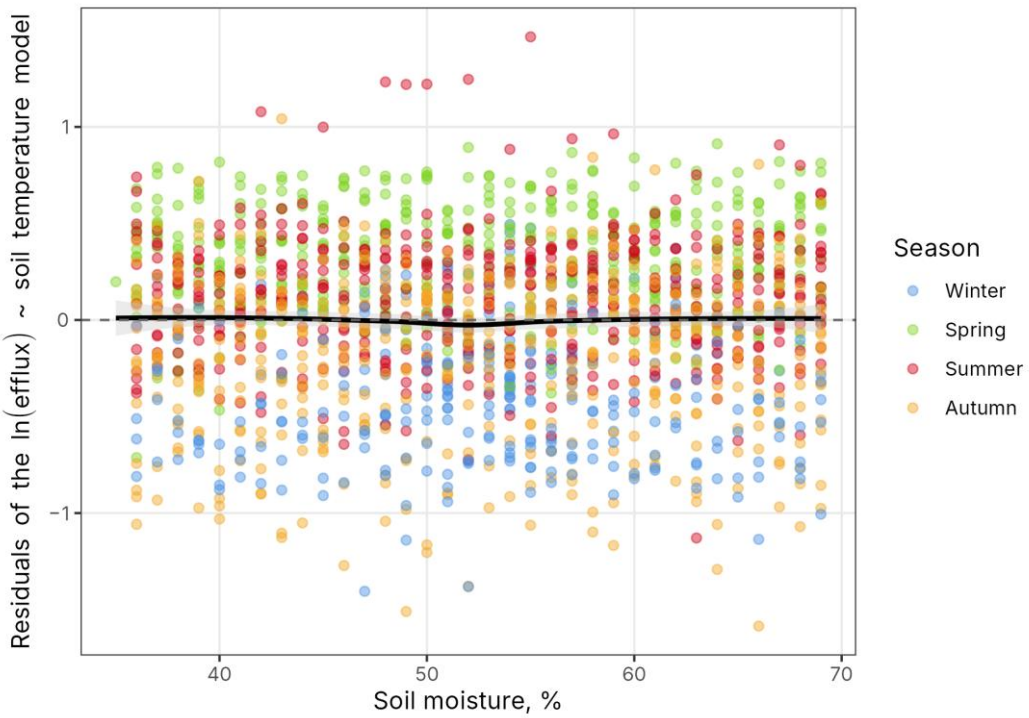


Figure 5. Dependence of the residuals of the temperature (Q_{10}) model of CO_2 emission on soil moisture. The black line is a LOESS smoother with its 95% confidence band (grey), and the dashed line marks zero residual.

3.3. Assessment of the Annual CO_2 Emission Budget for the Sirius Federal Territory

The annual soil respiration budget was estimated by summing monthly CO_2 fluxes, calculated as the product of the mean daily emission and the number of days in the month (sums based on medians are given for comparison).

In calculating the total annual flux within the territory's boundaries, it was taken into account that 64.27% of the Sirius FT's area consists of sealed surfaces (roads, buildings, and hard surfaces), which were conventionally excluded from the emission calculation. Thus, the active emitting area amounted to 35.73% of the total area, or 477.3 ha out of 1335.88 ha (the contour defined by Federal Law No. 437-FZ, excluding water bodies). The sealed fraction (64.27%) was estimated from a Sentinel-2B image of 24 May 2025 using an NDVI threshold combined with OpenStreetMap layers (the mapping is described in a separate manuscript under review). Unpaved roads and the gravel beach were not measured and are included in the unsealed area.

The annual CO_2 flux per unit of unsealed area was 1744 g C m^{-2} yr^{-1} (95% bootstrap CI 1601–1920), or 1684 g C m^{-2} yr^{-1} when based on medians (95% CI 1546–1800). The total annual carbon flux from the unsealed part of the territory was about 8322 t C yr^{-1} (7642–9164), equivalent to 30,514 t CO_2 yr^{-1} (28,021–33,601). At sealed fractions of 60% and 70%, the total would be 9316 and 6987 t C yr^{-1}, respectively. The largest contributions to the annual budget came from the summer months: June (198 g C m^{-2} $month^{-1}$, 11.4%), July (259 g C m^{-2} $month^{-1}$, 14.9%) and August (235 g C m^{-2} $month^{-1}$, 13.5%). Together, the summer months accounted for 39.7% of the annual budget, whereas the winter period (December–February) contributed 11.7% (Figure 6). The interpolated January contributed 71 g C m^{-2} (4.1%), and replacing it with the December or February value changed the annual flux by 0.7% (about 13 g C m^{-2}). The 11 measured months alone summed to about 1670 g C m^{-2}.

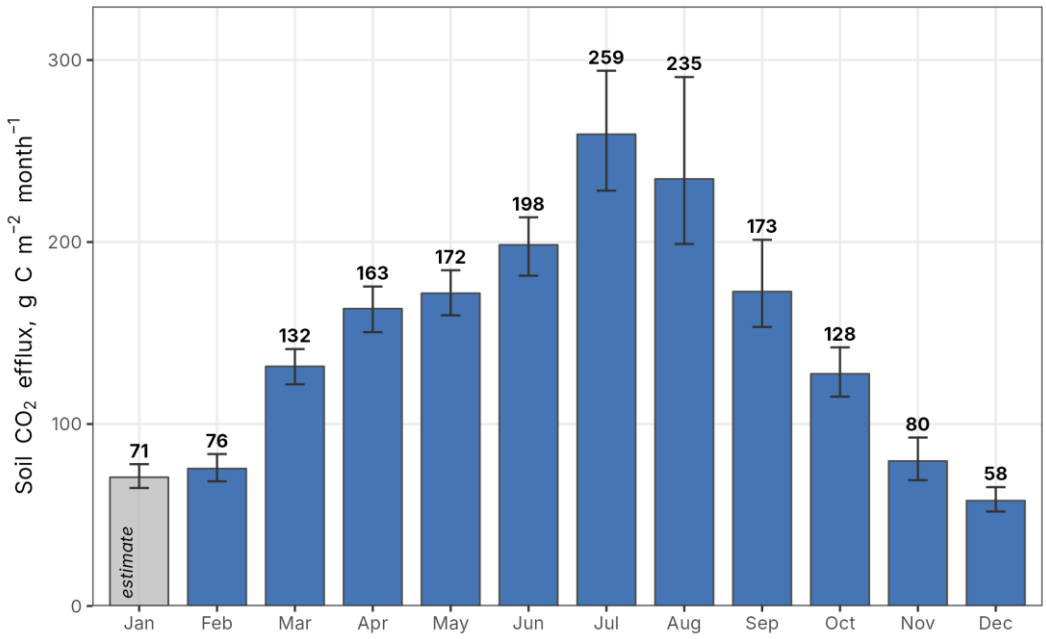


Figure 6. Monthly contribution to the annual CO_2 emission budget (January is estimated by interpolation. Error bars are 95% bootstrap confidence intervals).

3.4. Seasonal Variation in Between-Site Dispersion of Soil CO_2 Efflux

To characterize how differences among the 11 monitoring sites changed over the annual cycle, the dispersion of monthly median CO_2 efflux among sites was evaluated for the 11 measured months. In absolute terms, it was largest in July (IQR 1.68, SD 1.72, range 5.77 g C m^{-2} day^{-1}) and smallest in winter (range 1.56 g C m^{-2} day^{-1} in December). A Friedman test on absolute deviations from the monthly across-site median indicated significant variation ($\chi^2 = 19.9$, df = 10, $p = 0.03$), and the July–December contrast was significant (Wilcoxon $p = 0.0098$).

However, absolute dispersion closely followed the monthly mean flux (Spearman $\varrho = 0.93$, $p < 0.001$, $n = 11$ months). Scale-free measures did not show a warm-season increase: the coefficient of variation of site medians ranged from 13.9% (March) to 26.8% (November) and was highest in the cold months, and the standard deviation of ln-transformed site medians varied between 0.14 (May) and 0.25 (November). Applying the Friedman test to absolute deviations of ln-transformed medians gave $\chi^2 = 9.8$, df = 10, $p = 0.46$, and the July–December contrast was not significant (Wilcoxon $p = 0.32$). We therefore conclude that the larger absolute differences among sites in summer reflect the scaling of dispersion with mean flux, and that there is no evidence of a seasonal change in relative between-site differentiation in this dataset.

3.5. Relationship of Soil CO_2 Efflux with Soil Properties and Mowing Regime

Soil organic carbon, SOC stock, pH, bulk density, and the content of rock fragments were available for all 11 sites (Table 2). Site mean fluxes (mean of monthly means, February–December) were not significantly related to any of these properties (Spearman $|\varrho| \leq 0.52$, $p \geq 0.10$, $n = 11$), nor to mowing regime (Kruskal–Wallis $p = 0.33$, $n = 4$, 4 and 3 sites). The strongest relationships were a positive one with the content of rock fragments in the 0–10 cm layer ($\varrho = 0.52$, $p = 0.10$) and a negative one with the SOC stock ($\varrho = -0.46$, $p = 0.15$). Mean flux was 4.53, 5.53 and 4.88 g C m^{-2} day^{-1} at sites that were not mown, mown once a month and mown more than twice a month, respectively. Q_{10} was also unrelated to soil properties ($|\varrho| \leq 0.21$, $p \geq 0.54$). Restricting the analysis to the nine sites with the pit within 25 m of the measurement points gave the same result ($|\varrho| \leq 0.43$, $p \geq 0.24$). With 11 sites,

statistical power is low, so these results show only that no strong relationship was detectable and do not exclude moderate effects. MS-1 had the highest SOC stock (15.1 kg m^{-2}) and a high SOC content in the 0–10 cm layer (5.03%) but the lowest flux, and MS-2, the site with the highest topsoil SOC (6.45%), did not have an elevated flux. We therefore treat the explanations offered for between-site differences as hypotheses.

4. Discussion

4.1. Seasonal Dynamics and Temperature Control of Emission

As noted above, a unimodal pattern of seasonal CO_2 emission dynamics was identified, with a maximum in July and a minimum in December. Overall, this pattern does not differ fundamentally from patterns established for soils of temperate and subtropical climates. A similar seasonal trend, with a maximum in the summer months and a minimum in winter, has been described for urban forests in Beijing (where a Q_{10} model explained 76% of emission variance) [29], for urban lawns in Hefei in the subtropical zone of China [30], and for soils of urban ecosystems in the central Chernozem region of Russia [8]. This supports the widely recognized role of temperature as the main control of seasonal soil respiration across climates, consistent with the fundamental principles set out by Lloyd and Taylor [31] and with later studies of the global carbon cycle [32]. At the same time, the humid subtropical setting of the Sirius FT is expressed less in the shape of the seasonal curve than in its duration: the median flux in December (1.75 g C m^{-2} day^{-1}) was still about 22% of the July value, and fluxes remained substantial throughout the cold season in the absence of a frost period.

The pooled Q_{10} coefficient (1.48, 95% CI 1.42–1.55) lies in the lower part of the range typical of soil ecosystems on a global scale (median Q_{10} ~2.23) and below the global mean value, estimated at ~2.4 [32]. The relatively moderate temperature sensitivity observed under the humid subtropical conditions of the Imeretinskaya Lowland is consistent with the notion that, under conditions of persistently high moisture and the absence of prolonged freezing periods, microbial communities become adapted to functioning within a narrow temperature range, which in turn constrains the magnitude of Q_{10}. According to a global meta-analysis, Q_{10} is negatively correlated with mean annual temperature (MAT): a 1 °C increase in MAT leads to an approximately 2.27% decrease in Q_{10} [32]. For a humid subtropical region with a mean annual temperature of about 14–16 °C, expected Q_{10} values would be approximately 1.7–2.0. Our value is lower than predicted from MAT. Similar values (Q_{10} = 1.48–1.65) have been recorded for urban lawns in subtropical Hefei [30]. Lower Q_{10} values in warm, humid climates are to be expected: in the absence of prolonged temperature stress, microbial communities function within a relatively narrow and stable range of conditions, which limits their temperature sensitivity [32,33].

Within the study area, the Q_{10} coefficient varied among sites in the range of 1.35–1.65. The lowest values were found at MS-7 (1.35) and MS-3 (1.37), and the highest at geoplastically transformed sites (MS-10: 1.62, MS-11: 1.65). With the present design, differences among sites cannot be attributed to a particular factor, and the confidence intervals of site-specific Q_{10} overlap widely.

The Q_{10} values reported here are apparent temperature sensitivities. When month was included in the model, the relationship between flux and soil temperature within months was absent ($Q_{10} \approx 1.01$, $p = 0.79$), indicating that the estimate largely reflects the seasonal covariation of flux with temperature, which also includes changes in root activity and plant phenology [34]. Repeated measurements at the same sites in consecutive months are autocorrelated (lag-1 residual correlation 0.58), which inflates the nominal precision of ordinary regression. Mixed models and cluster-robust errors gave wider intervals around the same estimate, so the conclusion of a moderate Q_{10} is unaffected. In addition, time of day was not controlled and was partly confounded with site. Including the

air-temperature proxy for time of day did not change relative differences among sites (flux at MS-1 remained about 28–29% lower than at the other sites) but increased the pooled Q_{10} slightly (1.51 versus 1.48). The small chamber area (78 cm^2) also limits the representation of tussock-forming grasses at a single point.

The absence of a significant correlation between soil moisture and emission distinguishes the study area from steppe urban ecosystems, where moisture acts as a limiting factor. In Rostov-on-Don, for example, emission activity increased with increasing soil moisture, with peak values observed at 20–30% moisture content [16]. In urban soils of the steppe zone of Russia (Kursk), moisture was found to be the primary factor controlling CO_2 emission during the summer period (r = 0.44–0.50, $p < 0.05$) [8]. Under the humid subtropical conditions of the Imeretinskaya Lowland, where annual precipitation was high (1613 mm in 2025) and peaks in autumn–winter, with no pronounced dry season, soils experience virtually no moisture deficit. At the intensively managed lawns (MS-6 to MS-8), regular irrigation further reduces the likelihood of water deficit. Thus, moisture here remains consistently within a range that does not limit microbial activity within the observed range of 35–69%, which is consistent with data for urban soils in Moscow [14] and for urban lawns in the subtropical zone of Australia [35], where high soil moisture throughout the year does not create water stress for microorganisms.

The absence of a detectable moisture effect should be interpreted with three limitations in mind. First, moisture was recorded as point readings at the time of measurement and does not describe the moisture of the whole rooting zone. Second, the sampled range (35–69%) did not include strongly dry or waterlogged conditions, so the nonlinear responses reported for such extremes could not be detected. Third, moisture and temperature covary seasonally, so part of a moisture effect could be absorbed by the temperature term. The moisture term remained non-significant in the mixed model and within sites, which supports the conclusion that moisture did not limit efflux across the range observed in 2025.

In summary, the Sirius dataset shows a temperature-related seasonal cycle with moderate Q_{10} and no detectable moisture limitation. In this setting, a humid subtropical climate that keeps soils moist and unfrozen throughout the year coexists with a mosaic of recently transformed and, in part, irrigated soils; the climatic and anthropogenic controls therefore cannot be separated with the present design, and the data are best used as an integrated reference for this type of urban ecosystem. In 2025, the annual precipitation at the nearest station was 1613 mm, and the mean annual air temperature was 15.1 °C (Section 2.1). A single year of observation does not allow interannual variability to be assessed, so the reported fluxes should be regarded as representative of 2025.

4.2. Comparison with Urban Ecosystems of Other Climatic Zones and Annual Budget

Comparing the observed emission values with those reported for other climatic zones serves not merely to catalogue similarities and differences in magnitude, but to examine how climate context—temperature regime, moisture availability and the length of the biologically active period—shapes both the magnitude and the seasonal expression of soil respiration across urban ecosystems. The median daily CO_2 emission values for the studied sites (3.69–6.16 g C m^{-2} day^{-1} over the year) allow the study area to be compared with CO_2 flux data from urban soils in other cities across different climatic zones. Such comparisons are inherently approximate because studies differ in measurement methods, chamber type, measurement season, land cover, and sampling design; they are therefore used here to position the Sirius dataset relative to other urban ecosystems rather than to test differences statistically. Annual values are compared with annual values and growing-season values with growing-season values. For the Sirius FT, the mean flux for April–

October was 6.2 g C m^{-2} day^{-1} (4.5 at MS-1, the site with the lowest flux), and the annual mean flux was 4.8 g C m^{-2} day^{-1}

Temperate climate. Mean growing-season values for lawns in Moscow are approximately 5.0 g C m^{-2} day^{-1}, and for areas with woody vegetation, 2.7–4.5 g C m^{-2} day^{-1} [14,36]. For a mixed urban forest in Beijing, values of 1.7–3.8 g C m^{-2} day^{-1} have been recorded [29]. The growing-season mean flux of the Sirius sites (6.2 g C m^{-2} day^{-1}, and 4.5 at the lowest-flux site MS-1) is higher than values for Moscow lawns (about 5.0) and at or above the upper end of the values for wooded areas in Moscow and Beijing.

Steppe zone. Comparison with soils in Rostov-on-Don [15] is particularly informative, since a number of soils in the Imeretinskaya Lowland were formed from migration-segregation Chernozems used as parent material. Urban soils in Rostov-on-Don are characterized by an emission range of 2–6 g C m^{-2} day^{-1} [15], similar in magnitude to the annual median fluxes of the Sirius FT despite the markedly different climate. Because soil properties and measurement periods differ among studies, we draw no conclusion about the influence of parent material.

Subtropical and tropical climate. Mean seasonal values from urban lawns in Australia reach 7–12 g C m^{-2} day^{-1} [35,37], and for tropical urban soils under lawns in Singapore, mean annual emission was 7.7 g C m^{-2} day^{-1} [38]. Both the growing-season mean (6.2) and the annual mean (4.8 g C m^{-2} day^{-1}) of the Sirius FT are lower than these values. At MS-10, the flux was highest in July–September. Geoplastic transformation, proximity to water bodies, and management may influence fluxes in urban soils [14,39], but these factors cannot be separated with the present design, and irrigation is documented only for MS-6 to MS-8.

Within the limits of such comparisons, the fluxes observed in the Sirius FT fall between those typically reported for temperate urban ecosystems and those reported for warmer subtropical and tropical cities. Although the study area is located at approximately 43°24′ N, its climate is humid subtropical (Cfa according to the Köppen classification), which is unusual in the Russian context. This is related to the moderating influence of the Black Sea, which accumulates heat, and to the barrier effect of the Greater Caucasus, which limits the penetration of cold air masses from the north. The internal variability among sites (from 3.69 to 6.16 g C m^{-2} day^{-1} on an annual basis, i.e., a 1.7-fold spread) is comparable to differences between functional zones within a single city, as shown for Seoul, Boston, and Kursk [8,40,41]. Taken together, the climatic setting (mild winters, absence of a freezing period, and a year-round biologically active period) and the recent history of soil transformation make the Sirius FT an informative case for soil CO_2 efflux in a humid subtropical urban ecosystem. The dataset presented here (twice-monthly measurements at 11 sites over eleven months, together with the annual flux estimate and its seasonal distribution) is intended as a reference for comparison with urban ecosystems in other climatic and soil-anthropogenic settings, bearing in mind that it covers a single year.

Scaling the results to an annual basis allows comparison of the data obtained with global estimates of the urban carbon balance. The annual CO_2 flux from the unsealed portion of the Sirius FT was 1744 g C m^{-2} yr^{-1} (1.74 kg C m^{-2} yr^{-1}, 95% CI 1.60–1.92). For comparison, under the temperate-cold climate of Quebec (Canada), annual emissions from urban lawns ranged from 0.5 to 2.0 kg C m^{-2} yr^{-1}, depending on the mowing regime [42]. In Boston (temperate climate, mean annual temperature ~10 °C), emissions from urban lawns during the growing season, scaled to an annual basis, were about 0.9–1.1 kg C m^{-2} yr^{-1} [40]. Under the monsoonal climate of Seoul (mean annual temperature 12.5 °C, precipitation 1450 mm yr^{-1}), annual emissions from urban soils ranged from 0.48 to 1.45 kg C m^{-2} yr^{-1} depending on land-use type. The highest values were recorded for mixed forests (1.45 ± 0.11 kg C m^{-2} yr^{-1}), while for urban lawns the annual flux value was 1.05 ± 0.09 kg C m^{-2} yr^{-1}, with 43–56% of the annual budget occurring during the summer period [41].

The mean annual CO_2 flux from soils in Singapore (mean annual temperature 27.4 °C, precipitation 2358 mm yr^{-1}) was approximately 0.92 kg C m^{-2} yr^{-1} [43]. Higher annual values at the Sirius FT than in these temperate cities are likely related, at least in part, to the longer biologically active period under humid subtropical conditions, in contrast to Moscow, where soil respiration is strongly reduced during several cold months; however, differences in land cover (including irrigated and managed lawns), measurement methodology, and annual scaling procedure also contribute.

The total annual flux from the unsealed portion of the territory (477.3 ha) was 8322 t C yr^{-1} (7642–9164), or 30,514 t CO_2 yr^{-1} (28,021–33,601). The permanent resident population of the Sirius Federal Territory (14,448 inhabitants on 1 January 2025) [44] is below the minimum population threshold of 50,000 inhabitants used to delineate "urban centres" in global urban emission inventories such as the GHS Urban Centre Database (GHS-UCDB R2024A) [45], thereby precluding a direct population-matched comparison at the urban-centre level. We therefore compared per-capita flux intensities instead. Normalized to the resident population, the estimated soil CO_2 flux corresponds to 2.11 t CO_2 per capita yr^{-1}, equivalent to approximately 66% of the median per-capita anthropogenic CO_2 emissions reported for Russian urban centres in the smallest population class resolvable in this database (50,000–100,000 inhabitants; n = 121; median 3.20 t CO_2 per capita yr^{-1}; IQR: 2.61–4.32). This comparison should nevertheless be interpreted cautiously, because the registered resident population substantially understates the effective population using the territory, given its function as an Olympic and resort infrastructure zone with a large transient visitor population. Consequently, a comparison based on registered residents alone is likely to overestimate the relative contribution of soil CO_2 flux. Furthermore, the two flux types differ fundamentally in their sources, spatial boundaries, and accounting frameworks; the resulting comparison should therefore be regarded as indicative rather than as a precise estimate of the contribution of soil respiration to anthropogenic CO_2 emissions.

The annual estimate should be treated as an order-of-magnitude figure for the unsealed surfaces of the territory. First, the 11 sites are park and recreational plots, many of them managed lawns, and were selected purposively. The estimate is applied to the whole unsealed area (477.3 ha), although unsealed land also includes unpaved roads and the gravel beach, which were not measured, and may include other cover types that were not sampled. Second, the sealed fraction (64.27%) was estimated from a satellite image of 24 May 2025, and the budget changes by about +12% to −16% across the 60–70% range. Third, measurements were made at twice-monthly daytime visits without recording the time of day, so diel variation is not resolved. Fourth, January was interpolated, although its influence on the annual total was small (0.7%). Finally, the estimate covers one year only.

It should be emphasized that the assumption of zero emission from sealed surfaces is somewhat conditional. A number of studies have recorded residual CO_2 fluxes through asphalt and concrete surfaces. Studies have shown that SOC content beneath impervious surfaces may amount to 35–62% of the content in surface soils of open areas [46]. Furthermore, microbial activity and the mineralization of organic matter continue beneath asphalt and concrete surfaces, albeit at a reduced intensity [47]. This implies that the actual annual budget for the territory may be somewhat higher than the estimate presented here.

4.3. Differences Among Sites and Their Seasonality

Annual median fluxes of nine of the 11 sites were similar despite contrasting soil histories, vegetation and management, which suggests that, under a long biologically active period and no detectable moisture limitation, such differences are weakly expressed in annual fluxes. This remains a hypothesis, since no relationship with the measured soil properties was detected (Section 3.5) and other factors were not measured. Two sites differed consistently. After adjustment for month, flux at MS-1 (shaded, non-intervention)

was 25% lower and at MS-10 39% higher than the all-site geometric mean. The MS-1 difference remained when the proxy for time of day was included (29% lower than the other ten sites with the proxy, 28% without it), so it is unlikely to be a sampling-order artefact. Persistent canopy shading is one candidate explanation among several that cannot be separated here [48,49]. MS-10 had the highest fluxes, especially in July–September, when it was also the most variable. Its history of geoplasty and proximity to a water body are candidate explanations that cannot be tested with the present data.

Management is a further confounding factor. The sites differ in mowing frequency, and the three regimes (no mowing, mowing once a month, mowing more than twice a month) did not differ in mean flux (Kruskal–Wallis $p = 0.33$) or in Q_{10}. Irrigation, fertilizers, and fungicides were applied at MS-6, MS-7, and MS-8, which are also the sites mown most often, so their effects cannot be separated from that of mowing. The fluxes of these three sites were within the range of the nine sites with similar flux, so we found no sign of a strong effect of irrigation or fertilization on the annual flux, although three sites are not sufficient for testing it. No irrigation schedule was kept, and the measurements were not linked to irrigation events. Clippings were left on the soil surface at most sites. Management is also confounded with soil origin and age, since the youngest soil (MS-6) was established in 2024. With 11 purposively selected sites, we therefore cannot attribute differences or similarities to any single management practice and make no such inference.

The apparent seasonal widening of absolute differences among sites arises from the scaling of dispersion with mean flux, and relative differences were not larger in the warm season. We therefore do not interpret it as a seasonal change in spatial heterogeneity, and the dataset does not support this inference. A practical point follows: when sites are compared in absolute units, summer months will always show the largest contrasts, which should be borne in mind when designing monitoring schemes.

5. Conclusions

Soil CO_2 efflux in the park and recreational areas of the Sirius Federal Territory exhibited a pronounced unimodal seasonal cycle, with the highest flux in July and the lowest in December. Soil temperature was the principal abiotic correlate of temporal variation in CO_2 efflux, whereas soil moisture did not significantly constrain respiration under the observed humid subtropical conditions. The pooled Q_{10} of 1.48 indicates moderate temperature sensitivity of soil respiration, which largely reflects the seasonal cycle.

The estimated annual CO_2 flux from the unsealed portion of the Sirius Federal Territory reached 8322 t C yr^{-1} (30,514 t CO_2 yr^{-1}, 95% CI 28,021–33,601), with 39.7% of the annual flux occurring during summer and only 11.7% during winter. This seasonal concentration of soil CO_2 release highlights the importance of accounting for the duration of the biologically active period when estimating urban soil carbon fluxes.

The Sirius Federal Territory combines a humid subtropical coastal climate that is unusual in the Russian context, shaped by the Black Sea and the Greater Caucasus, with rapid and extensive anthropogenic transformation of the soil cover during 2008–2014. In this setting, twice-monthly, replicated measurements at 11 sites across almost the entire annual cycle provide a reference dataset of soil CO_2 efflux for a humid subtropical urban ecosystem, which can be used for comparison with urban ecosystems under contrasting climatic and land-use conditions.

Differences among sites were small relative to seasonal variation and were due mainly to two sites (MS-1 lower, MS-10 higher). Absolute differences among sites were larger in summer, but they scaled with mean flux and did not indicate a seasonal change in relative between-site differentiation.

Taken together, the results characterize soil CO_2 efflux in a humid subtropical urban ecosystem with recently and strongly transformed soils as a seasonal flux that is primarily

related to soil temperature, has a moderate Q_{10}, and remains substantial throughout a long biologically active period. The dataset provides a reference for comparison with urban ecosystems in other climatic and land-use settings. Absolute differences among sites scale with mean flux, which should be taken into account when comparing sites in absolute units.

Supplementary Materials: The following supporting information can be downloaded at: https://www.mdpi.com/article/10.3390/soilsystems10120154/s1. Figure S1. Diagnostics of the mixed-effects model of the temperature dependence of soil CO_2 efflux: (a) normal Q–Q plot of residuals, (b) residuals versus fitted values of ln(efflux); Table S1. Monthly mean (SD) of soil CO_2 efflux by site, g C m^{-2} day^{-1} (n = 14 per cell). January was not measured and is not included (for the annual budget it was estimated as the mean of December and February); Table S2. Dominant plant species at the monitoring sites.

Author Contributions: P.N.S.—Conceptualization, formal analysis, investigation, writing—original draft preparation; S.N.G.—supervision, project administration, writing—review and editing, funding acquisition; I.P.L.—investigation, data curation; S.S.T., K.A.T.—methodology, investigation; N.V.S.—writing—review and editing; M.O.K.—investigation, writing—review and editing. All authors have read and agreed to the published version of the manuscript.

Funding: This research was funded by the grant of the state program of the "Sirius" Federal Territory "Scientific and technological development of the "Sirius" Federal Territory" (Agreement No. 3-03 dated 18 February 2025).

Institutional Review Board Statement: Not applicable.

Informed Consent Statement: Not applicable.

Data Availability Statement: The datasets generated during and/or analyzed during the current study are available from the corresponding author on reasonable request.

Conflicts of Interest: The authors declare no conflicts of interest.

Abbreviations

The following abbreviations are used in this manuscript:

BD	bulk density
CI	confidence interval
CO_2	carbon dioxide
FT	Federal Territory
GAM	generalized additive model
IQR	interquartile range
LMM	linear mixed-effects model
MAT	mean annual temperature
MS	monitoring site
RF	rock fragments
SD	standard deviation
SOC	soil organic carbon
SRC	Soil Respiration Chamber
WRB	World Reference Base for Soil Resources
Q_{10}	temperature coefficient

References

1. Lou, Y.; Li, Z.; Zhang, T.; Liang, Y. CO_2 emissions from subtropical arable soils of China. *Soil Biol. Biochem.* **2004**, *36*, 1835–1842. https://doi.org/10.1016/j.soilbio.2004.05.006.
2. Tuffa, S.; Hoag, D.; Treydte, A.C. Effects of clipping and irrigation on carbon storage in grasses: Implications for CO_2 emission mitigation in rangelands. *Carbon Manag.* **2018**, *9*, 177–186. https://doi.org/10.1080/17583004.2018.1451963.

3. Iqbal, J.; Hu, R.; Lin, S.; Ahamadou, B.; Feng, M. Carbon dioxide emissions from Ultisol under different land uses in mid-subtropical China. *Geoderma* **2009**, *152*, 63–73. https://doi.org/10.1016/j.geoderma.2009.05.011.
4. van Delden, L.; Rowlings, D.W.; Scheer, C.; De Rosa, D.; Grace, P.R. Effect of urbanization on soil methane and nitrous oxide fluxes in subtropical Australia. *Glob. Change Biol.* **2018**, *24*, 5695–5707. https://doi.org/10.1111/gcb.14444.
5. Kelsey, K.C.; Wickland, K.P.; Striegl, R.G.; Neff, J.C. Variation in soil carbon dioxide efflux at two spatial scales in a topographically complex boreal forest. *Arct. Antarct. Alp. Res.* **2012**, *44*, 457–468. https://doi.org/10.1657/1938-4246-44.4.457.
6. Cai, Y.; Sawada, K.; Hirota, M. Spatial variation in forest soil respiration: A systematic review of field observations at the global scale. *Sci. Total Environ.* **2023**, *874*, 162348. https://doi.org/10.1016/j.scitotenv.2023.162348.
7. Vasenev, V.I.; Stoorvogel, J.J.; Vasenev, I.I. Urban soil organic carbon and its spatial heterogeneity in comparison with natural and agricultural areas in the Moscow region. *Catena* **2013**, *107*, 96–102. https://doi.org/10.1016/j.catena.2013.02.009.
8. Sarzhanov, D.A.; Vasenev, V.I.; Vasenev, I.I.; Sotnikova, Y.L.; Ryzhkov, O.V.; Morin, T. Carbon stocks and CO_2 emissions of urban and natural soils in Central Chernozemic region of Russia. *Catena* **2017**, *158*, 131–140. https://doi.org/10.1016/j.catena.2017.06.021.
9. Wu, X.; Yuan, J.; Ma, S.; Feng, S.; Zhang, X.; Hu, D. Seasonal spatial pattern of soil respiration in a temperate urban forest in Beijing. *Urban For. Urban Green.* **2015**, *14*, 1122–1130. https://doi.org/10.1016/j.ufug.2015.10.009.
10. Jian, J.; Steele, M.K. Heterogeneity of soil CO_2 efflux from local parks across an urban landscape. *Landsc. Ecol.* **2024**, *39*, 16. https://doi.org/10.1007/s10980-024-01812-4.
11. Alía, T.; González-Ubierna, S.; Sánchez-Jiménez, A.; Abad-Calderón, R.; Casermeiro, M.Á. Soil moisture as the dominant driver of CO_2 efflux in Mediterranean urban green spaces: Evidence for a Gaussian temperature response and mechanistic modelling of moisture and temperature interactions. *SOIL* **2026**, *12*, 915–935. https://doi.org/10.5194/soil-12-915-2026.
12. Ryndin, A.V.; Kozin, V.K. Assessment of agroclimatic resources of mountainous regions of the Russian subtropics. *Tr. Kuban. Gos. Agrar. Univ.* **2008**, *4*, 97–101. (In Russian)
13. Vyshkvarkova, E.; Voskresenskaya, E.; Martin-Vide, J. Spatial distribution of the daily precipitation concentration index in Southern Russia. *Atmos. Res.* **2018**, *203*, 36–43. https://doi.org/10.1016/j.atmosres.2017.12.003.
14. Vasenev, V.; Varentsov, M.; Konstantinov, P.; Romzaykina, O.; Kanareykina, I.; Dvornikov, Y.; Manukyan, V. Projecting urban heat island effect on the spatial-temporal variation of microbial respiration in urban soils of Moscow megalopolis. *Sci. Total Environ.* **2021**, *786*, 147457. https://doi.org/10.1016/j.scitotenv.2021.147457.
15. Gorbov, S.N.; Vasenev, V.I.; Minaeva, E.N.; Tagiverdiev, S.S.; Skripnikov, P.N.; Bezuglova, O.S. Short-Term Dynamics of CO_2 Emission and Carbon Content in Urban Soil Structures in the Steppe Zone. *Eurasian Soil Sci.* **2023**, *56*, 1270–1280. https://doi.org/10.1134/S1064229323601282.
16. Gorbov, S.N.; Terekhov, I.V.; Bezuglova, O.S.; Tagiverdiev, S.S.; Skripnikov, P.N.; Nosov, G.N.; Vasenev, V.I. Long-Term Dynamics of Carbon Emission in Artificial Soils under Urban Lawns in the Steppe Zone Conditions. *Eurasian Soil Sci.* **2025**, *58*, 67. https://doi.org/10.1134/S1064229324603913.
17. Shcherbina, V.G.; Shcherbina, Y.G.; Volkov, A.N. Plant communities of the Imeretinskaya Lowland. *Bull. P. P. Ershov Ishim State Pedagog. Inst.* **2013**, *6*, 140–147. (In Russian)
18. Sukhorukov, D.V.; Tregubov, O.V. The potential of the natural and climatic conditions of the Imeretinskaya Lowland for the introduction of tropical plants. *Lesotekhnicheskiy Zhurnal (For. Eng. J.)* **2014**, *4*, 61–68. https://doi.org/10.12737/8441. (In Russian)
19. Zakharikhina, L.V.; Malyukova, L.S.; Ryndin, A.V. Genesis and geochemistry of the soils of urban landscapes of the Black Sea coast of Russia. *Catena* **2022**, *210*, 105881. https://doi.org/10.1016/j.catena.2021.105881.
20. Rogozhina, E.V.; Vasileyko, M.V. Experience in studying the physicochemical properties and biological activity of soils of recreational zones in Sochi. *Subtrop. Ornam. Hortic.* **2020**, *74*, 179–186. https://doi.org/10.31360/2225-3068-2020-74-179-186. (In Russian)
21. Rogozhina, E.V.; Zakharikhina, L.V. Oligotrophy of microbial community and CO_2 emission dynamics in yellow soils under conditions of anthropogenesis (on the example of Sochi). *Subtrop. Ornam. Hortic.* **2022**, *81*, 161–171. https://doi.org/10.31360/2225-3068-2022-81-161-171. (In Russian)
22. Rogozhina, E.V.; Zakharikhina, L.V. Transformation of physicochemical properties and CO_2 emission of urban soils in the mountainous landscape of Sochi. *Eurasian Soil Sci.* **2025**, *58*, 620–633. https://doi.org/10.1134/S1064229324603810.
23. Weather and Climate (Pogoda i Klimat). Adler Airport, WMO 37171, Archive of Observations for 2025. Available online: http://www.pogodaiklimat.ru/history/37171.htm (accessed on 5 November 2026).
24. Balabanov, I.P.; Nikiforov, S.P.; Pashkovsky, I.S. *The Imeretinskaya Lowland. Natural and Geological Conditions, Development Challenges*; Nedra: Moscow, Russia, 2011; 281p. (In Russian)

25. IUSS Working Group WRB. *World Reference Base for Soil Resources. International Soil Classification System for Naming Soils and Creating Legends for Soil Maps*, 4th ed.; International Union of Soil Sciences (IUSS): Vienna, Austria, 2022.
26. Madalina, V.; Valentina, C.; Natalia, E.; Lucian, L.; Monica, M.; Anda, R.; György, D. Experimental determination of carbon dioxide flux in soil and correlation with dependent parameters. *IOP Conf. Ser. Earth Environ. Sci.* **2020**, *616*, 012010. https://doi.org/10.1088/1755-1315/616/1/012010.
27. Bates, D.; Mächler, M.; Bolker, B.; Walker, S. Fitting linear mixed-effects models using lme4. *J. Stat. Softw.* **2015**, *67*, 1–48. https://doi.org/10.18637/jss.v067.i01.
28. Kuznetsova, A.; Brockhoff, P.B.; Christensen, R.H.B. lmerTest package: Tests in linear mixed effects models. *J. Stat. Softw.* **2017**, *82*, 1–26. https://doi.org/10.18637/jss.v082.i13.
29. Chen, W.; Jia, X.; Zha, T.; Wu, B.; Zhang, Y.; Li, C.; Wang, X.; He, G.; Yu, H.; Chen, G. Soil respiration in a mixed urban forest in China in relation to soil temperature and water content. *Eur. J. Soil Biol.* **2013**, *54*, 63–68. https://doi.org/10.1016/j.ejsobi.2012.10.001.
30. Tao, X.; Cui, J.; Dai, Y.; Wang, Z.; Xu, X. Soil respiration responses to soil physiochemical properties in urban different green-lands: A case study in Hefei, China. *Int. Soil Water Conserv. Res.* **2016**, *4*, 224–229. https://doi.org/10.1016/j.iswcr.2016.08.001.
31. Lloyd, J.; Taylor, J.A. On the temperature dependence of soil respiration. *Funct. Ecol.* **1994**, *8*, 315–323. https://doi.org/10.2307/2389824.
32. Chen, S.; Wang, J.; Zhang, T.; Hu, Z. Climatic, soil, and vegetation controls of the temperature sensitivity (Q_{10}) of soil respiration across terrestrial biomes. *Glob. Ecol. Conserv.* **2020**, *22*, e00955. https://doi.org/10.1016/j.gecco.2020.e00955.
33. Zheng, Z.M.; Yu, G.R.; Fu, Y.L.; Wang, Y.S.; Sun, X.M.; Wang, Y.H. Temperature sensitivity of soil respiration is affected by prevailing climatic conditions and soil organic carbon content: A trans-China based case study. *Soil Biol. Biochem.* **2009**, *41*, 1531–1540. https://doi.org/10.1016/j.soilbio.2009.04.013.
34. Davidson, E.A.; Janssens, I.A. Temperature sensitivity of soil carbon decomposition and feedbacks to climate change. *Nature* **2006**, *440*, 165–173. https://doi.org/10.1038/nature04514.
35. van Delden, L.; Larsen, E.; Rowlings, D.; Scheer, C.; Grace, P. Establishing turf grass increases soil greenhouse gas emissions in peri-urban environments. *Urban Ecosyst.* **2016**, *19*, 749–762. https://doi.org/10.1007/s11252-016-0529-1.
36. Sushko, S.; Ananyeva, N.; Ivashchenko, K.; Vasenev, V.; Kudeyarov, V. Soil CO_2 emission, microbial biomass, and microbial respiration of woody and grassy areas in Moscow (Russia). *J. Soils Sediments* **2019**, *19*, 3217–3225. https://doi.org/10.1007/s11368-018-2151-8.
37. Livesley, S.J.; Dougherty, B.J.; Smith, A.J.; Navaud, D.; Wylie, L.J.; Arndt, S.K. Soil-atmosphere exchange of carbon dioxide, methane and nitrous oxide in urban garden systems: Impact of irrigation, fertiliser and mulch. *Urban Ecosyst.* **2010**, *13*, 273–293. https://doi.org/10.1007/s11252-009-0119-6.
38. Velasco, E.; Segovia, E.; Choong, A.M.; Lim, B.K.; Vargas, R. Carbon dioxide dynamics in a residential lawn of a tropical city. *J. Environ. Manag.* **2021**, *280*, 111752. https://doi.org/10.1016/j.jenvman.2020.111752.
39. Chen, Y.; Day, S.D.; Shrestha, R.K.; Strahm, B.D.; Wiseman, P.E. Influence of urban land development and soil rehabilitation on soil–atmosphere greenhouse gas fluxes. *Geoderma* **2014**, *226–227*, 348–353. https://doi.org/10.1016/j.geoderma.2014.03.017.
40. Decina, S.M.; Hutyra, L.R.; Gately, C.K.; Getson, J.M.; Reinmann, A.B.; Gianotti, A.G.S.; Templer, P.H. Soil respiration contributes substantially to urban carbon fluxes in the greater Boston area. *Environ. Pollut.* **2016**, *212*, 433–439. https://doi.org/10.1016/j.envpol.2016.01.012.
41. Bae, J.; Ryu, Y. Spatial and temporal variations in soil respiration among different land cover types under wet and dry years in an urban park. *Landsc. Urban Plan.* **2017**, *167*, 378–385. https://doi.org/10.1016/j.landurbplan.2017.07.020.
42. Allaire, S.E.; Dufour-L'Arrivée, C.; Lafond, J.A.; Lalancette, R.; Brodeur, J. Carbon dioxide emissions by urban turfgrass areas. *Can. J. Soil Sci.* **2008**, *88*, 529–532. https://doi.org/10.4141/CJSS07043.
43. Ng, B.J.L.; Hutyra, L.R.; Nguyen, H.; Cobb, A.R.; Kai, F.M.; Harvey, C.; Gandois, L. Carbon fluxes from an urban tropical grass-land. *Environ. Pollut.* **2015**, *203*, 227–234. https://doi.org/10.1016/j.envpol.2014.06.009.
44. Krasnodarstat. *Krasnodar Krai. Statistical Yearbook. 2024*; Krasnodarstat: Krasnodar, Russia, 2025; Section 2.3, p. 13. (In Russian)
45. Marí Rivero, I.; Melchiorri, M.; Florio, P.; Schiavina, M.; Krasnodębska, K.; Politis, P.; Uhl, J.H.; Pesaresi, M.; Maffenini, L.; Sulis, P.; et al. *GHS-UCDB R2024A—GHS Urban Centre Database 2025 [Data Set]*; European Commission, Joint Research Centre (JRC): Ispra, Italy, 2025.
46. Skripnikov, P.N.; Gorbov, S.N.; Salnik, N.V.; Tagiverdiev, S.S.; Mezhenkov, A.A.; Bezuglova, O.S. Study of the content and stocks of carbon in soils of sealed territories in the core of the Rostov agglomeration. *Zhivye I Biokosnye Sist. (Living Bio-Inert Syst.)* **2025**, *53*, 10. https://doi.org/10.18522/2308-9709-2025-53-3. (In Russian)

47. Wang, Y.H.; Shi, Y.M.; Sun, G.D.; Li, J.T.; Chen, H.; Chow, A.T.; Yang, Z.B.; Majidzadeh, H.; Wang, J.J. Soil Organic Carbon Signature under Impervious Surfaces. *ACS Earth Space Chem.* **2020**, *4*, 1785–1792. https://doi.org/10.1021/acsearthspacechem.0c00174.
48. Zanchi, F.B.; Meesters, A.G.; Waterloo, M.J.; Kruijt, B.; Kesselmeier, J.; Luizão, F.J.; Dolman, A.J. Soil CO_2 exchange in seven pristine Amazonian rain forest sites in relation to soil temperature. *Agric. For. Meteorol.* **2014**, *192–193*, 96–107. https://doi.org/10.1016/j.agrformet.2014.03.009.
49. Jevon, F.V.; Gewirtzman, J.; Lang, A.K.; Ayres, M.P.; Matthes, J.H. Tree species effects on soil CO_2 and CH_4 fluxes in a mixed temperate forest. *Ecosystems* **2023**, *26*, 1587–1602. https://doi.org/10.1007/s10021-023-00852-2.

Disclaimer/Publisher's Note: The statements, opinions and data contained in all publications are solely those of the individual author(s) and contributor(s) and not of MDPI and/or the editor(s). MDPI and/or the editor(s) disclaim responsibility for any injury to people or property resulting from any ideas, methods, instructions or products referred to in the content.